

Oval shaped droplet solutions in the saturation process of some pattern formation problems

Xiaofeng Ren ^{*†}

Department of Mathematics
The George Washington University
Washington, DC 20052, USA

Juncheng Wei [‡]

Department of Mathematics
The Chinese University of Hong Kong
Hong Kong, PRC

November 28, 2008

Abstract

The first stage in the transition from a coarse structure to a fine structure in many pattern formation problems involves the change of a standard geometric object such as a round disc to a less standard geometric object such as an oval shaped set. On a generic domain two small oval shaped sets are found as solutions to a nonlocal geometric problem. This problem arises as the singular limit of both the Ohta-Kawasaki theory for diblock copolymers and the Gierer-Meinhardt theory for morphogenesis in cell development. The two sets have the same center which is a global minimum of the diagonal of the regular part of a Green's function. This minimum point may be regarded as a kind of center of the domain. Moreover the second derivatives of the regular part of the Green's function define a major axis and a minor axis for the domain. One of the oval shaped solutions is stable and it aligns itself along the major axis. The other oval shaped solution is unstable and is parallel to the minor axis.

1 Introduction

Fine, periodic structures are often preferred to coarse, single structures in many pattern formation problems. Examples include the Ohta-Kawasaki density functional theory for block copolymers [13] and the Gierer-Meinhardt theory for morphogenesis in cell development [6]. In the the Ohta-Kawasaki theory, the level of structure saturation is controlled by the strength of the long range interaction between polymer chains. In the Gierer-Meinhardt theory the diffusion coefficient of the inhibitor performs the same function.

The transition from a coarse structure to a fine structure is not well understood mathematically. Such a saturation process may contain several steps. As depicted in Figure 1, first a well known single object, like a round disc, deforms to a less standard structure, such as an elongated, oval shaped set. Then deformation continues and a neck appears on the set signaling splitting. Finally the structure breaks off to two disjoint pieces.

^{*}Corresponding author. Phone: 1 202 994-6791; Fax: 1 202 994-6760; E-mail: ren@gwu.edu

[†]Supported in part by NSF grants DMS-0509725, DMS-0754066.

[‡]Supported in part by an Earmarked Grant of RGC of Hong Kong.

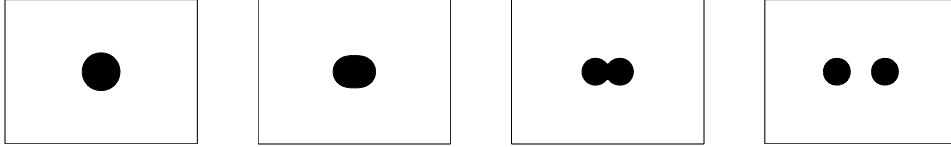


Figure 1: A round droplet deforms to an oval droplet, then to a necked droplet, before splits to two droplets.

Our study uses a nonlocal geometric model. We are given a smooth and bounded domain D in R^2 and two parameters $a \in (0, 1)$ and $\gamma > 0$. To each subset E of D with the prescribed size $|E| = a|D|$, where $|E|$ and $|D|$ are the Lebesgue measures of E and D respectively, we associate a free energy by

$$J(E) = P_D(E) + \frac{\gamma}{2} \int_D |(-\Delta)^{-1/2}(\chi_E - a)|^2 dx. \quad (1.1)$$

Here $P_D(E)$ is the perimeter of the part of the boundary of E that is inside D , i.e. the total length of the curves $\partial E \cap D$. The characteristic function χ_E of E is defined by $\chi_E(x) = 1$ if $x \in E$ and $\chi_E(x) = 0$ if $x \in D \setminus E$. The most interesting part in (1.1) is the nonlocal operator $(-\Delta)^{-1/2}$. From the $-\Delta$ operator on D with the Neumann boundary condition on ∂D , one obtains its inverse, $(-\Delta)^{-1}$ which is a nonlocal operator applied to functions on D with zero average, such as $\chi_E - a$. Our $(-\Delta)^{-1/2}$ is the positive square root of the operator $(-\Delta)^{-1}$.

If a subset E of D , satisfying $|E| = a|D|$, is a critical point of J and $\partial E \subset D$, there exists a number λ such that

$$H(\partial E) + \gamma(-\Delta)^{-1}(\chi_E - a) = \lambda, \quad \text{on } \partial E. \quad (1.2)$$

The constant λ is a Lagrange multiplier from the constraint $|E| = a|D|$, and $H(\partial E)$ is the curvature of the curve ∂E viewed from E .

The equation (1.2) arises from several problems. One of them is the Ohta-Kawasaki theory for diblock copolymers. In a diblock copolymer a molecule is a linear chain of an A-monomer block grafted covalently to a B-monomer block. Because of the repulsion between the unlike monomers, the different type sub-chains tend to segregate, but as they are chemically bonded in chain molecules, segregation of sub-chains cannot lead to a macroscopic phase separation. Only a local micro-phase separation occurs: micro-domains rich in A monomers and micro-domains rich in B monomers emerge as a result. A pattern formed from micro-domains is known as a morphology phase. Various phases, including lamellar, cylindrical, spherical, gyroid, etc, have been observed in experiments [1]. Figure 2 shows the spherical, cylindrical, and lamellar phases.

The free energy of a diblock copolymer melt proposed by Ohta and Kawakaki can be written on a bounded domain as

$$I(u) = \int_D \left[\frac{\epsilon^2}{2} |\nabla u|^2 + W(u) + \frac{\epsilon\gamma}{2} |(-\Delta)^{-1/2}(u - a)|^2 \right] dx \quad (1.3)$$

The relative density of the A monomers is u ; the relative density of the B monomers is $1 - u$. The function W is a balanced double well potential such as $(1/4)u^2(1 - u)^2$. Nishiura and Ohnishi identified (1.1) as a formal singular limit of the Euler-Lagrange equation of (1.3) [12]. Ren and Wei

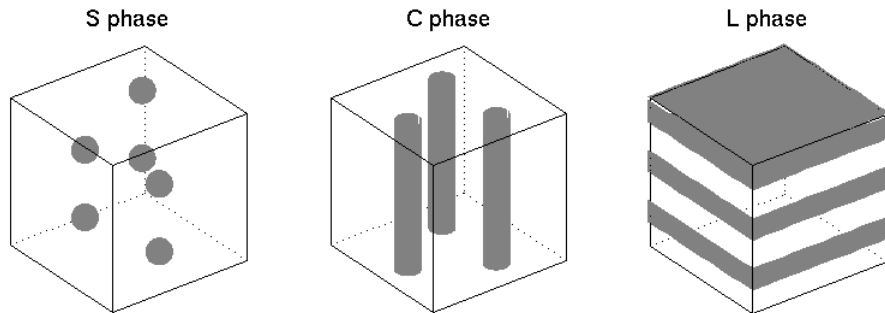


Figure 2: The spherical, cylindrical, and lamellar morphology phases commonly observed in diblock copolymer melts. The dark color indicates the concentration of type A monomers, and the white color indicates the concentration of type B monomers.

noted that (1.1) is the Γ -limit of (1.3) as ϵ tends to 0 [16], and hence put the convergence of I to its singular limit J under a rigorous mathematical framework. More studies on the lamellar phase of diblock copolymers, Figure 2 (3), may be found in [5, 18, 17, 3, 19, 23, 22, 2, 24, 25]. Solutions in three dimensions matching the spherical phase, Figure 2 (1), were found in [28]. More complex copolymer systems such as triblock copolymers and polymer blends were studied in [20, 21, 4].

A cross section of the cylindrical phase, Figure 2 (2), is a two dimensional domain D . The type A monomers form a subset E that is a union of many small droplets. The number of the droplets in a cross section is controlled by the parameter γ . The larger γ is, the more numerous and smaller the droplets are.

Another place where one finds (1.2) is the Gierer-Meinhardt theory for morphogenesis in cell development. It is a minimal model that provides a theoretical bridge between observations on the one hand and the deduction of the underlying molecular-genetic mechanisms on the other hand. Mathematically it is an activator-inhibitor type reaction-diffusion system with two unknowns of space variable $x \in D \subset \mathbb{R}^2$ and time variable $t > 0$. The first unknown, denoted by u describes the short-range autocatalytic substance, i.e., the activator, and the second unknown, denoted by v , is its long-range antagonist, i.e., the inhibitor. They satisfy the equations

$$u_t = \epsilon^2 \Delta u - u + \frac{u^p}{(1 + \kappa u^p)v^q}; \quad v_t = d \Delta v - v + \frac{u^r}{v^s}. \quad (1.4)$$

Here u and v satisfy the Neumann condition on the boundary of D , i.e.

$$\partial_\nu u(x, t) = \partial_\nu v(x, t) = 0, \quad \forall x \in \partial D, \forall t > 0 \quad (1.5)$$

where ∂_ν is the outward normal derivative operator on the boundary of D .

Activator-inhibitor systems were studied by Turing [30]. They may be used to model animal coats and skin pigmentation, Figure 3. In Appendix A we give a formal justification for the convergence of steady states of (1.4) to solutions of (1.2).

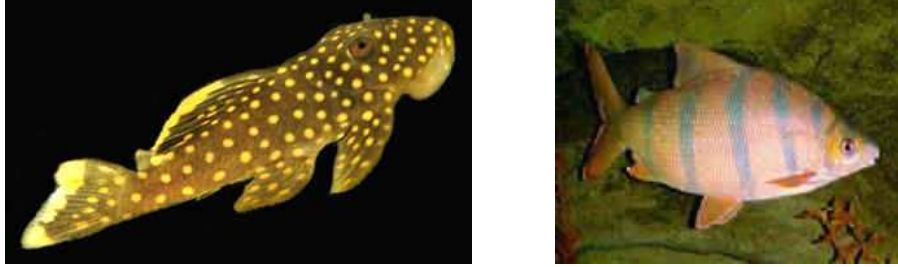


Figure 3: Spots on Gold Nugget Plecostomus and stripes on Distichodus Sexfasciatus.

In this paper we study the stage of the saturation process depicted in Figure 1 (2). We show that when a is sufficiently small and γ is in a particular range, on a generic domain there exist two solutions to (1.2), each of which has the shape of a small oval set. The location and direction of each oval droplet solution are determined via the regular part R of the Green's function of the domain D . The precise definition of R is given in (2.1). Note that the regular part $R(x, y) = R(x_1, x_2, y_1, y_2)$ is a function of two sets of variables $x \in D$ and $y \in D$, each of which has two components. The diagonal of R , given by $\tilde{R}(z) = R(z, z)$, is a function defined on D . If $z \rightarrow \partial D$, $\tilde{R}(z) \rightarrow \infty$. Hence \tilde{R} has at least one global minimum in D .

It is often convenient to use another parameter ρ in place of a . We set

$$\rho = \sqrt{\frac{a|D|}{\pi}}. \quad (1.6)$$

It is the average radius of a set E whose measure is fixed at $a|D|$. In other words if E were a round disc of the same measure $a|D|$, ρ would be the radius of E . The first stage of saturation occurs if γ is slightly greater than $\frac{12}{\rho^3}$. The number $\frac{12}{\rho^3}$ first emerged in the proof of an existence theorem for a round droplet solution in [27]. We will explain in Section 2 that it is the first point to avoid for the existence of the round droplet solution, and the stability of the round droplet solution changes as γ moves past it.

Our first result in this paper is the following.

Observation 1.1 *A vector $S \in \mathbb{R}^2$ is determined by the domain D via the second derivatives of R at a global minimum ζ of \tilde{R} . If $S \neq (0, 0)$, there exists $\delta > 0$ such that for each $c \in (12, 12 + \delta)$ there exists $\rho_0 > 0$ so that (1.2) admits two oval shaped droplet solutions, both centered at ζ , if $\gamma = \frac{c}{\rho^3}$ and $\rho < \rho_0$.*

Because of the symmetry $R(x, y) = R(y, x)$, $\frac{\partial R(z, z)}{\partial x_j} = \frac{\partial R(z, z)}{\partial y_j} = \frac{1}{2} \frac{\partial \tilde{R}(z)}{\partial z_j}$, $j = 1, 2$, and consequently

$$\frac{\partial R(\zeta, \zeta)}{\partial x_1} = \frac{\partial R(\zeta, \zeta)}{\partial x_2} = 0. \quad (1.7)$$

In some sense a global minimum of \tilde{R} is a center of D . Interestingly one can define a major axis

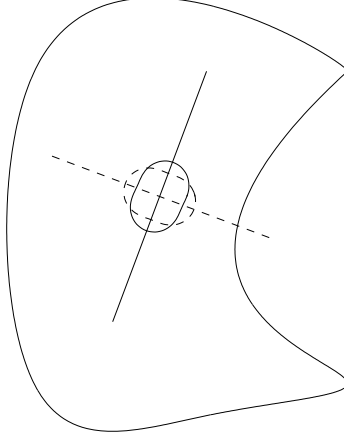


Figure 4: The solid line and the dashed line are the major and minor axes respectively. The stable oval droplet solution (in solid curve) is parallel to the major axis and the unstable oval droplet solution (in dashed curve) is parallel to the minor axis.

and a minor axis on a generic domain D . Let a vector $S = (S_1, S_2)$ be given by

$$S_1 = \frac{1}{2} \left(\frac{\partial^2 R(\zeta, \zeta)}{\partial x_1^2} - \frac{\partial^2 R(\zeta, \zeta)}{\partial x_2^2} \right), \quad S_2 = \frac{\partial^2 R(\zeta, \zeta)}{\partial x_1 \partial x_2} \quad (1.8)$$

The domain D is considered generic, or non-degenerate, with respect to ξ , if $(S_1, S_2) \neq (0, 0)$. In this case let σ be an angle such that

$$\cos 2\sigma = \frac{S_1}{|(S_1, S_2)|}, \quad \sin 2\sigma = \frac{S_2}{|(S_1, S_2)|}. \quad (1.9)$$

The minor axis is the line whose angle is σ and the major axis is the line whose angle is $\sigma + \frac{\pi}{2}$. The two oval droplets align themselves along the major and minor axes respectively, Figure 4.

Observation 1.2 *One of the two oval droplet solutions found in Observation 1.1 is stable and is parallel to the major axis whose angle is $\sigma + \frac{\pi}{2}$; the other oval droplet solution is unstable and is parallel to the minor axis whose angle is σ .*

If D is a rectangle with its length greater than its height, we found numerically that $S_1 < 0$ and $S_2 = 0$. Therefore $\sigma = \frac{\pi}{2}$ and $\sigma + \frac{\pi}{2} = \pi$. So the major axis is parallel to the length side and the minor axis is parallel to the height side. The two oval droplet solutions are depicted in Figure 5.

The degenerate case $S = (0, 0)$ is not covered in the two observations above. It occurs if for instance D is a disc or a perfect square. These two domains have no distinct major or minor axes.

Results similar to Observation 1.1 have appeared in many other problems in recent decades [7, 29, 14, 15], etc. To our knowledge, Observation 1.2 is new. It is the first result that links the direction of a solution to the shape of the domain via the second derivatives of R .

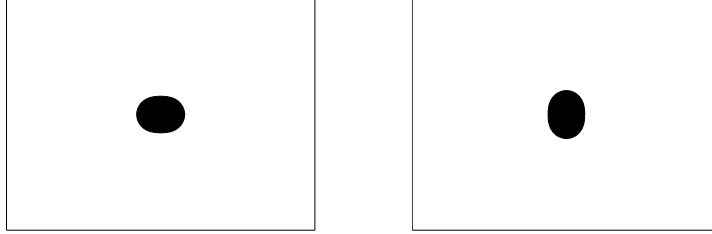


Figure 5: The domain D is $(0, 6) \times (0, 4)$ and $S = (-0.0118, 0)$ found numerically. The first droplet solution is stable while the second is unstable.

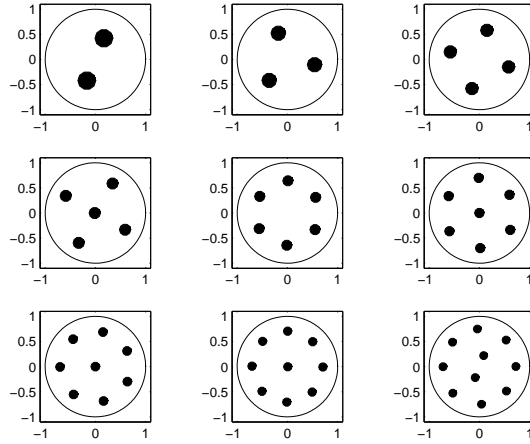


Figure 6: Round droplet solutions for $K = 2, 3, \dots, 10$.

This paper is organized as follows. Some existing results regarding round droplet solutions are recalled in Section 2. In Section 3 we describe the shape of an oval droplet, by identifying some bifurcation solutions of a rescaled version of (1.2) formulated on the entire plane R^2 . In Section 4, we study (1.2) on a bounded domain D and find two solutions with the shape of oval droplets. We also determine the location of these droplets. In Section 5, we show that the direction of the oval droplets must be either along the major axis or the minor axis of the domain. A few remarks are included in Section 6. The first appendix gives a formal derivation of (1.2) from the Gierer-Meinhardt system (1.4); the second appendix contains some technical calculations.

For simplicity we often write $e^{i\theta}$ for $(\cos \theta, \sin \theta)$, although no complex structure is used.

2 Round droplet solutions

Before we construct oval droplet solutions of (1.2), we recall some existing results about round droplet solutions. Let the Green's function of $-\Delta$ with the Neumann boundary condition be denoted by G .

It is a sum of two parts:

$$G(x, y) = \frac{1}{2\pi} \log \frac{1}{|x - y|} + R(x, y). \quad (2.1)$$

The regular part of $G(x, y)$ is $R(x, y)$. The Green's function satisfies the equation

$$-\Delta_x G(x, y) = \delta(x - y) - \frac{1}{|D|} \text{ in } D, \quad \partial_{\nu(x)} G(x, y) = 0 \text{ on } \partial D, \quad \int_D G(x, y) dx = 0 \text{ for } \forall y \in D.$$

Here Δ_x is the Laplacian with respect to the x -variable of G , and $\nu(x)$ is the outward normal direction at $x \in \partial D$. We set

$$F(\xi_1, \xi_2, \dots, \xi_K) = \sum_{k=1}^K R(\xi_k, \xi_k) + \sum_{k=1}^K \sum_{l=1, l \neq k}^K G(\xi_k, \xi_l), \quad (2.2)$$

for $\xi_k \in D$ and $\xi_k \neq \xi_l$ if $k \neq l$. Because $G(x, y) \rightarrow \infty$ if $|x - y| \rightarrow 0$ and $R(x, x) \rightarrow \infty$ if $x \rightarrow \partial D$, F admits at least one global minimum.

The first result shows the existence of a solution with a pattern of round droplets.

Theorem 2.1 ([26]) *Let $K \geq 1$ be an integer and*

$$\rho = \sqrt{\frac{a|D|}{K\pi}}. \quad (2.3)$$

1. *For every $\epsilon > 0$ there exists $\delta > 0$, depending on ϵ , K and D only, such that if*

$$\gamma\rho^3 \log \frac{1}{\rho} > 1 + \epsilon, \quad (2.4)$$

$$|\gamma\rho^3 - 2n(n+1)| > \epsilon n^2, \quad \text{for all } n = 2, 3, 4, \dots, \quad (2.5)$$

and

$$\rho < \delta, \quad (2.6)$$

then there exists a solution E of (1.2) which is a union of K disconnected components.

2. *Each component is close to a round disc whose radius is ρ .*

3. *Let the centers of these discs be $\zeta_1, \zeta_2, \dots, \zeta_K$. Then $\zeta = (\zeta_1, \zeta_2, \dots, \zeta_K)$, is a global minimum of the function F .*

The first condition (2.4) is an anti-coarsening condition. It prevents droplets from growing or shrinking. This condition is not needed if $K = 1$. The second condition (2.5) is known as the resonance condition, also called the gap condition. The next theorem shows that the stability of the droplet pattern depends on how (2.5) is satisfied.

Theorem 2.2 ([26]) *If (2.5) is satisfied because*

$$\gamma\rho^3 - 2n(n+1) < -\epsilon n^2, \quad \text{for all } n \geq 2, \quad (2.7)$$

then the round droplet solution is stable. Otherwise if (2.5) is satisfied but

$$\epsilon n^2 < \gamma\rho^3 - 2n(n+1), \quad \text{and } \gamma\rho^3 - 2(n+1)(n+2) < -\epsilon(n+1)^2 \quad (2.8)$$

for some $n \geq 2$, then the round droplet solution is unstable.

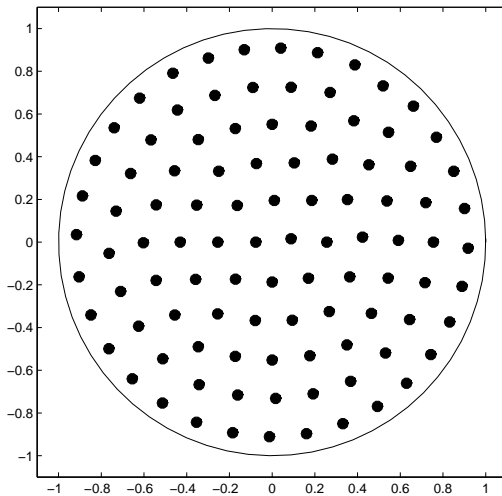


Figure 7: A round droplet solution with $K = 100$.

Figure 6 shows some round droplet solutions when D is a unit disc. The locations of the droplets are determined by numerically minimizing F of (2.2). Physicists believe that the droplets in a block copolymer must pack in a hexagonal pattern. This happens away from the boundary of D , if we take the number K of droplets to be large, Figure 7.

The single droplet case, i.e. $K = 1$, was treated in [27]. The three dimensional analogies of the two theorems were proved in [28]. Solutions there are unions of a number of small sets that are close to balls, Figure 2 (1).

The first resonance point in (2.5) is relevant to the saturation phenomenon we are studying in this paper. This is the first number 12 in the sequence $2n(n + 1)$ attained when $n = 2$. The round droplet solution changes from being stable to unstable when γ increases past $\frac{12}{\rho^3}$. We will find oval shaped droplet solutions when γ is near $\frac{12}{\rho^3}$.

3 The shape of an oval droplet

The shape of an the oval shaped object in an oval droplet solution is approximately determined by a solution of a problem in the entire plane R^2 .

We define a free energy functional

$$J_{R^2}(E) = P_{R^2}(E) + \frac{c}{2} \int_E \Gamma(\chi_E)(x) dx. \quad (3.1)$$

The functional (3.1) is used to model an enlarged droplet, so we impose the constraint

$$|E| = \pi. \quad (3.2)$$

The parameter $c > 0$ here is a scaled version of γ in (1.2). The periemter $P_{R^2}(E)$ of E in R^2 is the

length of ∂E . The operator Γ denotes the Newtonian potential operator given by

$$\Gamma(\chi_E)(x) = \int_{R^2} \frac{1}{2\pi} \left(\log \frac{1}{|x-y|} \right) \chi_E(y) dy. \quad (3.3)$$

The Euler-Lagrange equation of (3.1) is

$$H(\partial E) + c\Gamma(E) = \lambda, \text{ on } \partial E \quad (3.4)$$

where the constant λ is the Lagrange multiplier from the constraint $|E| = \pi$ on ∂E .

Consider sets that can be parametrized in the polar coordinates in the following way. There is a 2π periodic function u such that

$$E = \bigcup_{\theta \in [0, 2\pi]} \left(\bigcup_{r \in [0, \sqrt{1+u(\theta)}]} \{re^{i\theta}\} \right). \quad (3.5)$$

The requirement that $|E| = \pi$ implies that

$$\int_0^{2\pi} u(\theta) d\theta = 0, \quad (3.6)$$

for $|E| = \int_0^{2\pi} \int_0^{\sqrt{1+u(\theta)}} r dr d\theta = \int_0^{2\pi} \frac{1+u(\theta)}{2} d\theta = \pi$.

Obviously the unit disc $B(0, 1) = \{x \in R^2 : |x| < 1\}$, corresponding to $u = 0$, is a solution for any $c > 0$. The spectrum of the linearized operator of (3.4) at the unit disc was found in [27].

Lemma 3.1 ([27]) *The eigenvalues of the linearized operator at $B(0, 1)$ are*

$$\Lambda_{c,n} = \frac{n^2 - 1}{2} + \frac{c(1 - n)}{4n}, \quad n = 1, 2, 3, \dots$$

The corresponding eigenfunctions are $\cos n\theta$ and $\sin n\theta$.

Due to the translation invariance of this problem, one always has $\Lambda_{c,1} = 0$ with the eigenfunctions $\cos \theta$ and $\sin \theta$. We will only address stability modulo translation. The other eigenvalues, $\Lambda_{c,2}, \Lambda_{c,3}, \Lambda_{c,4}, \dots$, are all positive if $0 < c < 12$; when $c = 12$, $\Lambda_{12,2} = 0$. In general if $c = 2n(n+1)$ where $n = 2, 3, 4, \dots$, then $\Lambda_{2n(n+1),n} = 0$.

It is not too hard to see that all these $2n(n+1)$, $n = 2, 3, 4, \dots$, are bifurcation points. Let us treat the $n = 2$ case. The other cases can be dealt in a similar way. When $c = 2n(n+2) = 12$, $\Lambda_{12,2} = 0$. The eigenfunctions of $\Lambda_{12,2}$ are $\cos 2\theta$ and $\sin 2\theta$, both of which are π -periodic. We look for bifurcation solutions among π -periodic u 's of zero average. Such u 's are expanded as

$$u(\theta) = \sum_{j=1}^{\infty} (A_{2j} \cos 2j\theta + B_{2j} \sin 2j\theta). \quad (3.7)$$

It can be shown that the bifurcation diagram is of the generalized pitch-fork type, Figure 8. The diagram consists of a line and a surface that is similar to a paraboloid. The line represents the trivial solution $u = 0$ and the surface represents the bifurcation solutions. Whether the bifurcation solutions are stable depends on whether the paraboloid opens toward larger c direction (the super-critical case) or the smaller c direction (the sub-critical case). Numerical calculations suggest that it is the super-critical case. We make the following assumption in this paper.

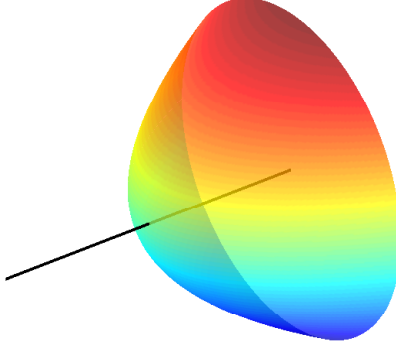


Figure 8: The bifurcation diagram when c is near 12.

Hypothesis 3.2 *The bifurcation diagram at $c = 12$ is super-critical. Hence the bifurcation solutions of (3.4) at $c = 12$ are stable.*

Following Hypothesis 3.2 we have $\delta > 0$ such that for each

$$c \in (12, 12 + \delta), \quad (3.8)$$

there exists a family of bifurcation solutions. Among this family one solution, which we denote by \tilde{u} , satisfies

$$A_2 > 0 \text{ and } B_2 = 0 \quad (3.9)$$

where A_2 and B_2 are the coefficients of $\cos 2\theta$ and $\sin 2\theta$ respectively in the expansion (3.7) of \tilde{u} . Then \tilde{u} has the form

$$\tilde{u} = d \cos 2\theta + \tilde{u}^\perp(\cdot, c, d), \quad (3.10)$$

where $d > 0$ and \tilde{u}^\perp is of order d^2 . We have denoted the A_2 coefficient of \tilde{u} by d . Other bifurcation solutions, with the same c value, are obtained from \tilde{u} by a rotation of angle Ω . We denote them by

$$u(\theta, \Omega) = \tilde{u}(\theta - \Omega). \quad (3.11)$$

Each solution $u(\cdot, \Omega)$ of (3.4) is degenerate since the linearized operator has a three dimensional kernel at u . The kernel is spanned by T_1 , T_2 , and P where

$$T_1(\theta, \Omega) = \sqrt{1 + u(\theta, \Omega)} \cos(\theta - \Omega), \quad T_2(\theta, \Omega) = \sqrt{1 + u(\theta, \Omega)} \sin(\theta - \Omega), \quad P(\theta, \Omega) = \frac{\partial u(\theta, \Omega)}{\partial \Omega}. \quad (3.12)$$

Geometrically T_1 and T_2 come from the translation invariance of the problem and P comes from the rotation invariance. More specifically place $u(\cdot, \Omega)$ in the equation (3.4) and differentiate the equation with respect to Ω . Then P appears as a member in the kernel.

To see T_1 and T_2 are also in the kernel, consider the solution \tilde{u} . Let us shift the set $E_{\tilde{u}}$ determined by the function \tilde{u} along the horizontal axis by $h \in R$. Denote the new set by $E^h = \{x \in R^2 :$

$x - (h, 0) \in E_{\tilde{u}}$. Let the boundary of E_h be parametrized by $v(\eta)$, $\eta \in [0, 2\pi]$, where $v(\eta)$ is 2π periodic and is related to $\tilde{u}(\theta)$ via

$$\sqrt{1+v(\eta)}e^{i\eta} = (h, 0) + \sqrt{1+\tilde{u}(\theta)}e^{i\theta}. \quad (3.13)$$

Inserting v into (3.4) and differentiating the equation with respect to h yield that $\frac{\partial v}{\partial h}\big|_{h=0}$ is in the kernel of the linearized operator. Implicit differentiation of (3.13) shows that

$$\begin{aligned} \begin{bmatrix} \frac{\partial \eta}{\partial \theta} & \frac{\partial \eta}{\partial h} \\ \frac{\partial v}{\partial \theta} & \frac{\partial v}{\partial h} \end{bmatrix} &= - \begin{bmatrix} \sqrt{1+v} \sin \eta & -\frac{\cos \eta}{2\sqrt{1+v}} \\ -\sqrt{1+v} \cos \eta & -\frac{\sin \eta}{2\sqrt{1+v}} \end{bmatrix}^{-1} \begin{bmatrix} \frac{\cos \theta}{2\sqrt{1+\tilde{u}}} \frac{\partial \tilde{u}}{\partial \theta} - \sqrt{1+\tilde{u}} \sin \theta & 1 \\ \frac{\sin \theta}{2\sqrt{1+\tilde{u}}} \frac{\partial \tilde{u}}{\partial \theta} + \sqrt{1+\tilde{u}} \cos \theta & 0 \end{bmatrix} \\ &= \begin{bmatrix} \frac{-\sin \eta}{\sqrt{1+v}} & \frac{\cos \eta}{\sqrt{1+v}} \\ 2\sqrt{1+v} \cos \eta & 2\sqrt{1+v} \sin \eta \end{bmatrix} \begin{bmatrix} \frac{\cos \theta}{2\sqrt{1+\tilde{u}}} \frac{\partial \tilde{u}}{\partial \theta} - \sqrt{1+\tilde{u}} \sin \theta & 1 \\ \frac{\sin \theta}{2\sqrt{1+\tilde{u}}} \frac{\partial \tilde{u}}{\partial \theta} + \sqrt{1+\tilde{u}} \cos \theta & 0 \end{bmatrix}. \end{aligned}$$

This implies that

$$\frac{\partial v}{\partial h}\big|_{h=0} = 2\sqrt{1+v(\eta)} \cos \eta\big|_{h=0} = 2\sqrt{1+\tilde{u}(\theta)} \cos \theta. \quad (3.14)$$

Therefore $\sqrt{1+\tilde{u}(\theta)} \cos \theta$ is in the kernel of the linearized operator at \tilde{u} . A similar argument with a shift of $E_{\tilde{u}}$ along the vertical direction shows that $\sqrt{1+\tilde{u}(\theta)} \sin \theta$ is also in the kernel. Finally a rotation by an angle Ω shows that T_1 and T_2 are in the kernel of the linearized operator at $u(\cdot, \Omega)$.

It follows from the fact that \tilde{u} has no $\sin 2\theta$ component that T_1 and T_2 are orthogonal. Since the integral of any π -periodic function multiplied by $\cos \theta$ or $\sin \theta$ is zero, T_j and P are orthogonal. Hence T_1, T_2 , and P form an orthogonal basis. Moreover T_1, T_2 , and P are all perpendicular to 1.

4 The location of an oval droplet

From now on we consider (1.2) on a bounded domain D with a small a . The profile determined by $u(\theta, \Omega)$ will be scaled down to become an approximate solution. We set

$$\gamma = \frac{c}{\rho^3}. \quad (4.1)$$

The constant c is fixed in the range $(12, 12+\delta)$ determined in (3.8), and ρ is a sufficiently small. As claimed in Observations 1.1 and 1.2, under Hypothesis 3.2 two oval shaped, droplet solutions will be found. One is stable and the other one is unstable.

If Hypothesis 3.2 were false, one could still find two oval droplet solutions, this time for $c \in (12-\delta, 12)$. However if this were to occur, the bifurcation diagram of (3.4) near $c = 12$ would be sub-critical. Consequently the two oval droplet solutions found on a bounded domain would be both unstable.

Given a subset E of D whose measure is fixed at $|E| = a|D| = \pi\rho^2$, in addition to the operators H and Γ given in Section 3, we define another operator R by

$$R(E)(x) = \int_E R(x, y) dy \quad (4.2)$$

where $R(x, y)$ is the regular part of the Green's function G (see (2.1)).

Let $\xi \in D$ be an arbitrary point and $w(\theta, \Omega) = \rho^2 u(\theta, \Omega)$. Define a set E_w by

$$E_w = \bigcup_{\theta \in [0, 2\pi]} \left(\bigcup_{r \in [0, \sqrt{\rho^2 + w(\theta)}]} \{\xi + r e^{i\theta}\} \right). \quad (4.3)$$

E_w is a scaled down version of E_u , centered at ξ . Note that $|E_w| = \pi \rho^2 = a|D|$. This set serves as an approximate solution. To find an exact solution, we perturb w by another zero average function ϕ to $w + \phi$. When acting on $E_{w+\phi}$, the operators H , Γ , and R are considered as operators on the function $w + \phi$. Then $w + \phi$ satisfies

$$H(w + \phi) + \gamma(\Gamma(w + \phi) + R(w + \phi)) = \text{Const}. \quad (4.4)$$

The equation (4.4) holds on the boundary of $E_{w+\phi}$. Since the boundary is parametrized by θ , $H(w + \phi)$, $\Gamma(w + \phi)$ and $R(w + \phi)$ are all functions of θ . Linearizing (4.4) and using the fact that $H(w) + \gamma\Gamma(w) = \text{Const.}$, we find that ϕ approximately satisfies

$$[H'(w) + \gamma\Gamma'(w)]\phi + \gamma R(w) \approx \text{Const}. \quad (4.5)$$

The linearized operator $H'(w) + \gamma\Gamma'(w)$ is self-adjoint and has the kernel spanned by T_1 , T_2 , and P . Three solvability conditions follow:

$$R(w) \perp T_j \quad (j = 1, 2) \text{ and } R(w) \perp P. \quad (4.6)$$

We use them to determine ξ and Ω .

To this end we expand $R(w)$ in terms of ρ : $R(w) = \sum_{k=0}^{\infty} \frac{\rho^k}{k!} \frac{\partial^k R}{\partial \rho^k} \Big|_{\rho=0}$. Calculations in Appendix B show that

$$R|_{\rho=0} = 0, \quad \frac{\partial R}{\partial \rho} \Big|_{\rho=0} = 0, \quad \text{and} \quad \frac{\partial^2 R}{\partial \rho^2} \Big|_{\rho=0} = 2\pi R(\xi, \xi).$$

Here $2\pi R(\xi, \xi)$ is a constant independent of θ . The first three terms in the expansion of $R(w)$ are all perpendicular to T_j and P , and no information can be deduced from them. The next order is

$$\frac{\partial^3 R}{\partial \rho^3} \Big|_{\rho=0} = 6\pi R_x(\xi, \xi) [\sqrt{1 + u(\theta)} e^{i\theta}].$$

We use $R_x(\xi, \xi)$ to denote the vector $(\frac{\partial R}{\partial x_1}, \frac{\partial R}{\partial x_2})$ of the two partial derivatives at the point (ξ, ξ) . The quantity $R_x(\xi, \xi) [\sqrt{1 + u} e^{i\theta}]$ is just the inner product of $R_x(\xi, \xi)$ and $\sqrt{1 + u} e^{i\theta}$. For a more consistent notation we view $R_x(\xi, \xi)$ as a linear functional and view the inner product as the result of the functional on the vector $\sqrt{1 + u} e^{i\theta}$. We also need to expand ξ in terms as ρ so that

$$\xi = \zeta + \rho\eta + \dots \quad (4.7)$$

where ζ and η are independent of ρ . Then

$$\frac{\partial^3 R}{\partial \rho^3} \Big|_{\rho=0} = 6\pi R_x[\sqrt{1 + u} e^{i\theta}] + \rho 6\pi R_{xx}[\eta, \sqrt{1 + u} e^{i\theta}] + \rho 6\pi R_{xy}[\sqrt{1 + u} e^{i\theta}, \eta] + O(\rho^2). \quad (4.8)$$

We have used the short hand notation

$$R_x = \left(\frac{\partial R(\zeta, \zeta)}{\partial x_1}, \frac{\partial R(\zeta, \zeta)}{\partial x_2} \right) \quad (4.9)$$

for the vector, and

$$R_{xx} = \begin{bmatrix} \frac{\partial^2 R(\zeta, \zeta)}{\partial x_1^2} & \frac{\partial^2 R(\zeta, \zeta)}{\partial x_1 \partial x_2} \\ \frac{\partial^2 R(\zeta, \zeta)}{\partial x_2 \partial x_1} & \frac{\partial^2 R(\zeta, \zeta)}{\partial x_2^2} \end{bmatrix}, \quad R_{xy} = \begin{bmatrix} \frac{\partial^2 R(\zeta, \zeta)}{\partial x_1 \partial y_1} & \frac{\partial^2 R(\zeta, \zeta)}{\partial x_1 \partial y_2} \\ \frac{\partial^2 R(\zeta, \zeta)}{\partial x_2 \partial y_1} & \frac{\partial^2 R(\zeta, \zeta)}{\partial x_2 \partial y_2} \end{bmatrix}. \quad (4.10)$$

for the matrices. $R_{xx}[\eta, \sqrt{1+ue^{i\theta}}]$ is the result of the matrix R_{xx} , considered as a bilinear form, acting on the vectors η and $\sqrt{1+ue^{i\theta}}$, and $R_{xy}[\sqrt{1+ue^{i\theta}}, \eta]$ is the result of the matrix R_{xy} acting on $\sqrt{1+ue^{i\theta}}$ and η .

Hence the ρ^3 order of $R(w)$ is

$$\frac{6\pi\rho^3}{3!} R_x[\sqrt{1+ue^{i\theta}}]. \quad (4.11)$$

Now examine the ρ^3 order terms in $\langle R(w), T_j \rangle = 0$ ($j = 1, 2$) and $\langle R(w), P \rangle = 0$. The last equation implies that

$$\langle R_x[\sqrt{1+ue^{i\theta}}], \frac{\partial u}{\partial \Omega} \rangle = 0, \quad (4.12)$$

which always holds since $\sqrt{1+u} \frac{\partial u}{\partial \Omega}$ is π -periodic, and the integral of any π -periodic function multiplied by $e^{i\theta}$ is 0.

The equation $\langle R_x[\sqrt{1+ue^{i\theta}}], T_1 \rangle = 0$ implies that

$$\int_0^{2\pi} (1+u)(R_{x_1}(\zeta, \zeta) \cos \theta + R_{x_2}(\zeta, \zeta) \sin \theta) \cos(\theta - \Omega) d\theta = 0.$$

Note that

$$\begin{aligned} \int_0^{2\pi} (1+u) \cos \theta \cos(\theta - \Omega) d\theta &= \int_0^{2\pi} (1+u) [\cos(\theta - \Omega) \cos \Omega - \sin(\theta - \Omega) \sin \Omega] \cos(\theta - \Omega) \\ &= \cos \Omega \|T_1\|_2^2 - \frac{\sin \Omega}{2} \langle 1+u, \sin 2(\theta - \Omega) \rangle = \cos \Omega \|T_1\|_2^2 \end{aligned}$$

where the last step follows from the fact that $\tilde{u}(\theta)$ has no $\sin 2\theta$ component. Similarly

$$\int_0^{2\pi} (1+u) \sin \theta \cos(\theta - \Omega) d\theta = \sin \Omega \|T_1\|_2^2. \quad (4.13)$$

We therefore obtain the consequence that

$$R_{x_1}(\zeta, \zeta) \cos \Omega + R_{x_2}(\zeta, \zeta) \sin \Omega = 0. \quad (4.14)$$

In a similar way the equation $\langle R(w), T_2 \rangle = 0$ implies that

$$-R_{x_1}(\zeta, \zeta) \sin \Omega + R_{x_2}(\zeta, \zeta) \cos \Omega = 0. \quad (4.15)$$

The equations (4.14) and (4.15) form a non-singular linear homogeneous system, so

$$R_{x_1}(\zeta, \zeta) = R_{x_2}(\zeta, \zeta) = 0. \quad (4.16)$$

Because of the symmetry $R(x, y) = R(y, x)$, (4.16) means that ζ is a critical point of the diagonal $\tilde{R}(z) = R(z, z)$. Since $\tilde{R}(z) \rightarrow \infty$ as $z \rightarrow \partial D$, the global minimum of \tilde{R} is attained in D . One can have ζ in (4.16) to be this minimum of \tilde{R} . This completes our justification of Observation 1.1.

5 The direction of an oval droplet

Calculations in Appendix B show that

$$\left. \frac{\partial^4 R}{\partial \rho^4} \right|_{\rho=0} = 12\pi R_{xx}(\xi, \xi)[\sqrt{1+ue^{i\theta}}, \sqrt{1+ue^{i\theta}}] + Const. \quad (5.17)$$

Because of (4.8) the ρ^4 order of $R(w)$ is

$$\frac{24\pi\rho^4}{4!}R_{xx}[\eta, \sqrt{1+ue^{i\theta}}] + \frac{24\pi\rho^4}{4!}R_{xy}[\sqrt{1+ue^{i\theta}}, \eta] + \frac{12\pi\rho^4}{4!}R_{xx}[\sqrt{1+ue^{i\theta}}, \sqrt{1+ue^{i\theta}}] + Const. \quad (5.18)$$

In the ρ^4 order of $\langle R(w), P \rangle$, since P is π -periodic, the inner products of P with the first two terms in (5.18) are 0. Hence we have

$$\langle R_{xx}[\sqrt{1+ue^{i\theta}}, \sqrt{1+ue^{i\theta}}], P \rangle = 0. \quad (5.19)$$

Let us set S_1 and S_2 by (1.8) and introduce $\sigma \in [0, 2\pi)$ so that

$$\cos 2\sigma = \frac{S_1}{\sqrt{S_1^2 + S_2^2}}, \quad \sin 2\sigma = \frac{S_2}{\sqrt{S_1^2 + S_2^2}}. \quad (5.20)$$

Note that

$$\begin{aligned} R_{xx}[e^{i\theta}, e^{i\theta}] &= R_{x_1x_1}(\zeta, \zeta) \cos^2 \theta + 2R_{x_1x_2}(\zeta, \zeta) \cos \theta \sin \theta + R_{x_2x_2}(\zeta, \zeta) \sin^2 \theta \\ &= \sqrt{S_1^2 + S_2^2} \cos 2(\theta - \sigma) + \frac{R_{x_1x_1} + R_{x_2x_2}}{2}. \end{aligned}$$

We claim that

$$\langle (1+u) \frac{R_{x_1x_1} + R_{x_2x_2}}{2}, P \rangle = 0. \quad (5.21)$$

This is because

$$\langle 1+u, P \rangle = \langle 1 + \tilde{u}(\theta - \Omega), -\tilde{u}'(\theta - \Omega) \rangle = - \int_0^{2\pi} (1 + \tilde{u}(\theta)) \tilde{u}'(\theta) d\theta = \left(\tilde{u} + \frac{\tilde{u}^2}{2} \right) \Big|_0^{2\pi} = 0.$$

Therefore (5.19) becomes

$$\langle (1+u) \cos 2(\theta - \sigma), P \rangle = 0, \quad \text{i.e. } \langle (1 + \tilde{u}(\theta - \Omega)) \cos 2(\theta - \sigma), -\tilde{u}'(\theta - \Omega) \rangle = 0.$$

A change of variable turns this to

$$- \int_0^{2\pi} (1 + \tilde{u}(\theta)) \tilde{u}'(\theta) \cos 2(\theta + \Omega - \sigma) d\theta = 0. \quad (5.22)$$

This equation determines Ω in terms of σ .

Finally we consider the inner products of (5.18) with T_j . The inner products of the third term in (5.18) and T_j are 0. We deduce

$$\langle R_{xx}[\eta, \sqrt{1+ue^{i\theta}}] + R_{xy}[\sqrt{1+ue^{i\theta}}, \eta], T_j \rangle = 0. \quad (5.23)$$

Arguing as in the last section we find that

$$(R_{x_1x_1} + R_{x_1y_1})\eta_1 + (R_{x_2x_1} + R_{x_1y_2})\eta_2 = 0, \quad (R_{x_1x_2} + R_{x_2y_1})\eta_1 + (R_{x_2x_2} + R_{x_2y_2})\eta_2 = 0. \quad (5.24)$$

By the the symmetry of R we deduce that

$$\frac{1}{2} \frac{\partial^2 \tilde{R}(\zeta)}{\partial z_1^2} = R_{x_1x_1} + R_{x_1y_1}, \quad \frac{1}{2} \frac{\partial^2 \tilde{R}(\zeta)}{\partial z_1 \partial z_2} = R_{x_2x_1} + R_{x_1y_2} = R_{x_1x_2} + R_{x_2y_1}, \quad \frac{1}{2} \frac{\partial^2 \tilde{R}(\zeta)}{\partial z_2^2} = R_{x_2x_2} + R_{x_2y_2}.$$

If ζ is a non-degenerate minimum of \tilde{R} , the linear system (5.24) is non-singular and

$$\eta = 0. \quad (5.25)$$

Recall $\gamma = \frac{c}{\rho^3}$. When c is close to 12, the equation (5.22) can be solved explicitly. In this case $\tilde{u}(\theta)$ is close to $d \cos 2\theta$ where d is a small positive constant and $\tilde{u}'(\theta)$ is close to $-2d \sin 2\theta$. We can approximately write (5.22) as

$$2d \int_0^{2\pi} \sin 2\theta \cos 2(\theta + \Omega - \sigma) d\theta = 0. \quad (5.26)$$

This implies that $\Omega = \sigma + \frac{n\pi}{2}$, $n = 0, 1, 2, \dots$. We have actually found two, not four, solutions. The first one corresponds to $\Omega = \sigma$ and the second one corresponds to $\Omega = \sigma + \frac{\pi}{2}$. Since \tilde{u} is π -periodic, we have the fact that

$$w(\cdot, \Omega) + \phi(\cdot, \Omega) = w(\cdot, \Omega + \pi) + \phi(\cdot, \Omega + \pi).$$

Therefore $\Omega = \sigma$ and $\Omega = \sigma + \pi$ represent the same solution; and $\Omega = \sigma + \frac{\pi}{2}$ and $\Omega = \sigma + \frac{3\pi}{2}$ also represent the same solution.

To determine the stability of the two solutions we study the dependence of the energy of $w + \phi$ on Ω . This energy of $w + \phi$ is close to the energy of w , and it suffices to consider

$$J(w) = P_D(\partial E_w) + \frac{\gamma}{2} \int_{E_w} \int_{E_w} \frac{1}{2\pi} \log \frac{1}{|x-y|} dx dy + \frac{\gamma}{2} \int_{E_w} \int_{E_w} R(x, y) dx dy, \quad (5.27)$$

in which only the third term depends on Ω . Hence we study the derivative of this term with respect to Ω

$$\frac{\partial J(w)}{\partial \Omega} = \frac{\gamma}{2} \frac{\partial}{\partial \Omega} \int_{E_w} \int_{E_w} R(x, y) dx dy = \frac{\gamma}{2} \int_0^{2\pi} R(w) \frac{\partial u}{\partial \Omega} d\theta. \quad (5.28)$$

The calculations of $R(w)$ and $\langle R(w), P \rangle$ earlier show that

$$\frac{\partial J(w)}{\partial \Omega} = \frac{\gamma \rho^2}{2} \int_0^{2\pi} R(w) \frac{\partial u}{\partial \Omega} d\theta = \frac{\gamma \rho^2}{2} \frac{\rho^4 \pi}{2} \int_0^{2\pi} -(1 + \tilde{u}(\theta)) \tilde{u}'(\theta) \cos 2(\theta + \Omega - \sigma) d\theta + O(\gamma \rho^7). \quad (5.29)$$

When c is close to 12, the above is approximated by

$$\frac{\partial J(w)}{\partial \Omega} \approx \frac{\gamma \rho^6 \pi}{4} \int_0^{2\pi} 2d \sin 2\theta \cos 2(\theta + \Omega - \sigma) d\theta = \frac{\gamma \rho^6 \pi^2}{2} (-d) \sin 2(\Omega - \sigma). \quad (5.30)$$

Note that $d > 0$. Hence the solution corresponding to $\Omega = \sigma$ gives a maximum of J with respect to Ω and therefore is unstable; the solution corresponding to $\Omega = \sigma + \frac{\pi}{2}$ gives a minimum of J with respect to Ω and therefore is stable.

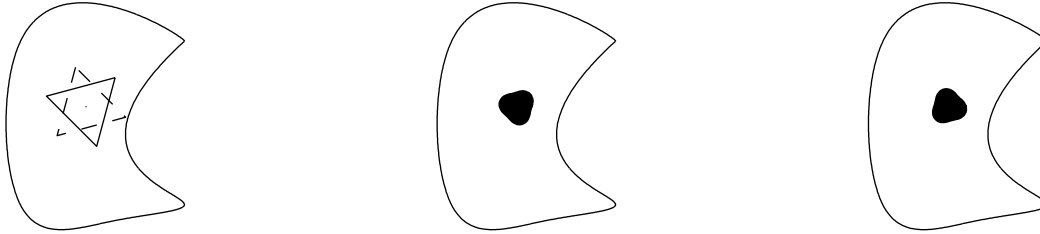


Figure 9: (1): The major triangle (solid line) and the minor triangle (dashed line) for a general domain. (2) and (3): Two triangular droplet solutions corresponding to the two triangles.

6 Discussion

If Hypothesis 3.2 can be confirmed, then using a type of Lyapunov-Schmidt reduction procedure we can prove Observations 1.1 and 1.2 rigorously. If Hypothesis 3.2 is false, we can still prove Observations 1.1 and 1.2 for c in the range $(12 - \delta, 12)$, although the two oval droplet solutions are both unstable.

We have only considered the first resonance point $c = 12$ corresponding to $n = 2$. One can also study higher resonance points $c = 2n(n + 1)$, for $n = 3, 4, \dots$. The solutions found near those resonance points are all unstable. Nevertheless these solutions are quite interesting.

Consider the $n = 3$ case first. The shape of a non-circular, droplet solution for γ close to $\frac{2n(n+1)}{\rho^3} = \frac{24}{\rho^3}$ looks like a triangle with corners smoothed out. As in Section 3, if we denote the profile by \tilde{u} , then $\tilde{u}(\theta) \approx d \cos 3\theta$. Instead of axes one can define two triangles on a generic domain D with the help of the third order derivatives of R . One of them can be termed the major triangle and the other the minor triangle. A rotation by $\frac{\pi}{3}$ turns one triangle to the other, Figure 9 (1). There should be two triangular droplet solutions on a generic D . One is in the direction of the major triangle of D and the other is in the direction of the minor triangle of D , Figure 9 (2) and (3).

For a general n , when γ is close to $\frac{2n(n+1)}{\rho^3}$, there should be two n -polygon shaped (with smoothed corners), droplet solutions on a generic D . The profile is given by $\tilde{u}(\theta) \approx d \cos n\theta$. The n -th order derivatives of R define two n -polygons for D . The two n -polygon droplets are parallel to the two n -polygons of D respectively.

The existence of a stable oval droplet solution and an unstable oval droplet solution indicates a type of imperfect bifurcation near the first resonance point $\frac{12}{\rho^3}$. However to understand the solution diagram completely near $\frac{12}{\rho^3}$, one must consider (1.2) with a small ρ for all c near 12. This is a harder problem than the one studied in this paper, since in Observation 1.1 the number ρ_0 in the restriction $\rho < \rho_0$ depends on $c \in (12, 12 + \delta)$. One will have to derive results for $\rho < \rho_0$ that hold uniformly with respect to c in a neighborhood of 12.

This paper only addresses the first stage of saturation, namely the deformation to an elongated shape from a round shape. A complete saturation theory will contain at least two more stages of transformation: appearance of necked droplets and breaking off of necked droplets. On the other hand, the opposite of saturation is simpler and much better understood. The Lifshitz-Slyozov-Wagner theory [9, 31] for the Ostwald ripening phenomenon describes how in a pattern of many droplets, some droplets grow larger while others shrink and disappear. This theory has been formulated mathematically by Niethammer [10, 11].

Kolokolnikov, Ward and Wei [8] have shown that oval shaped droplets appear as time dependent solutions in dynamic problems. The shape of a dynamic oval is similar to the one discussed here. However the oval direction there is not determined by the domain geometry. Instead it is related to the motion of the oval.

A The reduction of the Gierer-Meinhardt system

In this section we derive a singular limit for (1.4). The diffusion coefficient ϵ^2 of the variable u must be small: $0 < \epsilon \ll 1$. The diffusion coefficient of v must be large in the sense that $d = \frac{d_0}{\epsilon}$ where $d_0 > 0$ is independent of ϵ . Saturation in this problem is controlled by d_0 . The smaller d_0 is, the finer the pattern becomes. Moreover in the second equation of (1.4) we take $\iota = 0$. This case is known as the fast inhibitor limit.

The nonlinearity in the first equation of (1.4) is denoted by

$$f(u, v) = -u + \frac{u^p}{(1 + \kappa u^p)v^q}. \quad (\text{A.1})$$

It has a cubic shape with respect to u . For each $v > 0$, there exist three zeros of $f(u, v)$ as a function of u . There is a particular value v_0 such that at $v = v_0$, $f(\cdot, v_0)$ becomes a balanced cubic nonlinearity, in the sense $\int_0^z f(u, v_0) du = 0$. Here z is the largest zero of $f(\cdot, v_0)$.

We expect the u variable to develop a pattern shortly after the system (1.4) is started. A subset E of D emerges so that $u(x, t)$ is close to z in the set E and close to 0 in the set $D \setminus E$. The boundary of E in D is a collection of curves which we denote by Γ . The value of u changes abruptly across Γ .

The boundary Γ changes in time and we denote it by $\Gamma(\tau)$ where τ is a slow time variable so that $\tau = \epsilon^2 t$. Away from $\Gamma(\tau)$ we take $u \approx z\chi_E$ where χ_E is the characteristic function of E . The shape of u near $\Gamma(\tau)$ is more complicated. Let $Q(\xi, s)$ be the traveling wave solution of the problem

$$Q_{\xi\xi} + c(s)Q_{\xi} + f(Q, s) = 0, \quad \xi \in (-\infty, \infty). \quad (\text{A.2})$$

In (A.2), s is a parameter. As ξ tends to $-\infty$, we require that $Q(\xi, s)$ tend to 0, and as ξ tends to ∞ , we require that $Q(\xi, s)$ tend to the largest zero of $f(\cdot, s)$. The constant $c(s)$ is the velocity of the traveling wave. It is unknown and must be determined from the equation (A.2).

Let $d(x, \tau)$ be the signed distance function from a point x to $\Gamma(\tau)$. The sign of $d(x, \tau)$ is positive if x is in the set E and negative if x is in $D \setminus E$. We assume that approximately

$$u(x, t) \approx Q\left(\frac{d(x, \epsilon^2 t)}{\epsilon}, s\right) \quad (\text{A.3})$$

where s is constant, discussed later. Insert this Q into the first equation in (1.4) to find

$$\epsilon Q_{\xi} d_{\tau} = Q_{\xi\xi} |\nabla d|^2 + \epsilon Q_{\xi} \Delta d + f(Q, s).$$

It is known that on the set $\Gamma(\tau)$, $|\nabla d| = 1$ and $\Delta d(x, \tau) = H(x, \tau)$ where $H(x, \tau)$ is the curvature of $\Gamma(\tau)$ at x , viewed from E . Therefore we obtain

$$Q_{\xi\xi} + (\epsilon H - \epsilon d_{\tau}) Q_{\xi} + f(Q, s) = 0. \quad (\text{A.4})$$

Comparing (A.4) to (A.2) we deduce

$$c(s) = \epsilon H - \epsilon d_\tau. \quad (\text{A.5})$$

Note that d_τ is the normal velocity of the boundary $\Gamma(\tau)$ at the slow time τ , which we denote by $V(\tau)$: $V(\tau) = d_\tau$.

Now we discuss $c(s)$. On the boundary $\Gamma(\epsilon^2 t)$, s must be equal to $v(x, t)$. However unlike $u(x, t)$, $v(x, t)$ changes slowly in x . Asymptotically we have the expansion $v(x, t) \approx v_0 + \epsilon w(x, t)$, so that $c(s) = c(v) \approx c(v_0) + \epsilon c'(v_0)w$. Since v_0 is the point where $f(\cdot, v_0)$ is balanced, $c(v_0) = 0$. Hence (A.5) implies that

$$V = H - c'(v_0)w. \quad (\text{A.6})$$

It remains to find an equation for w . In the second equation in (1.4) (with $\iota = 0$) we deduce

$$\frac{d_0}{\epsilon} \Delta(v_0 + \epsilon w(x, t) - (v_0 + \epsilon w(x, t))) + \frac{u^r}{(v_0 + \epsilon w(x, t))^s} = 0.$$

As $\epsilon \rightarrow 0$, we find

$$d_0 \Delta w - v_0 + \frac{z^r}{v_0^s} \chi_E = 0 \quad (\text{A.7})$$

The equations (A.6) and (A.7) form a system for the evolution of the boundary Γ :

$$V = H - c'(0)w \text{ on } \Gamma, \quad d_0 \Delta w - v_0 + \frac{z^r}{v_0^s} \chi_E = 0 \text{ in } D. \quad (\text{A.8})$$

Note that the Neumann boundary condition for v implies the same boundary condition for w and hence

$$\int_D (-v_0 + \frac{z^r}{v_0^s} \chi_E) dx = 0.$$

Therefore $|E| = \frac{v_0^{s+1}}{z^r} |D|$. Define

$$a = \frac{v_0^{s+1}}{z^r}, \quad \gamma = -\frac{c'(v_0)z^r}{d_0 v_0^s}. \quad (\text{A.9})$$

A steady state satisfies $V = 0$. Then (A.8) becomes (1.2).

B Expansion of $R(w)$

Recall that

$$R(w)(\theta) = \int_{E_w} R(\xi + \rho \sqrt{1+u} e^{i\theta}, y) dy = \int_0^{2\pi} \int_0^{\rho \sqrt{1+u(\omega)}} R(\xi + \rho \sqrt{1+u(\theta)} e^{i\theta}, \xi + t e^{i\omega}) t dt d\omega.$$

Here the dependence of u on Ω is unimportant and hence not indicated.

Differentiation shows that

$$\begin{aligned} \frac{\partial R}{\partial \rho} &= \int_0^{2\pi} R(\xi + \rho \sqrt{1+u(\theta)} e^{i\theta}, \xi + \rho \sqrt{1+u(\omega)} e^{i\omega}) (1+u(\omega)) \rho d\omega \\ &\quad + \int_{E_w} R_x(\xi + \rho \sqrt{1+u(\theta)} e^{i\theta}, y) [\sqrt{1+u(\theta)} e^{i\theta}] dy. \end{aligned} \quad (\text{B.1})$$

From now on it is understood that in $\sqrt{1+ue^{i\theta}}$, u is a function of θ and in $\sqrt{1+ue^{i\omega}}$, u is a function of ω . Differentiation of (B.1) shows that

$$\begin{aligned}
\frac{\partial^2 R}{\partial \rho^2} &= \int_0^{2\pi} R(\xi + \rho\sqrt{1+ue^{i\theta}}, \xi + \rho\sqrt{1+ue^{i\omega}})(1+u(\omega)) d\omega \\
&+ 2 \int_0^{2\pi} R_x(\xi + \rho\sqrt{1+ue^{i\theta}}, \xi + \rho\sqrt{1+ue^{i\omega}})[\sqrt{1+ue^{i\theta}}](1+u(\omega))\rho d\omega \\
&+ \int_0^{2\pi} R_y(\xi + \rho\sqrt{1+ue^{i\theta}}, \xi + \rho\sqrt{1+ue^{i\omega}})[(1+u)^{3/2}e^{i\omega}]\rho d\omega \\
&+ \int_{E_w} R_{xx}(\xi + \rho\sqrt{1+ue^{i\theta}}, y)[\sqrt{1+ue^{i\theta}}, \sqrt{1+ue^{i\theta}}] dy.
\end{aligned} \tag{B.2}$$

Next

$$\begin{aligned}
\frac{\partial^3 R}{\partial \rho^3} &= 3 \int_0^{2\pi} R_x(\xi + \rho\sqrt{1+ue^{i\theta}}, \xi + \rho\sqrt{1+ue^{i\omega}})[\sqrt{1+ue^{i\theta}}](1+u(\omega)) d\omega \\
&+ 2 \int_0^{2\pi} R_y(\xi + \rho\sqrt{1+ue^{i\theta}}, \xi + \rho\sqrt{1+ue^{i\omega}})[(1+u)^{3/2}e^{i\omega}] d\omega \\
&+ 3 \int_0^{2\pi} R_{xx}(\xi + \rho\sqrt{1+ue^{i\theta}}, \xi + \rho\sqrt{1+ue^{i\omega}})[\sqrt{1+ue^{i\theta}}, \sqrt{1+ue^{i\theta}}](1+u(\omega))\rho d\omega \\
&+ 2 \int_0^{2\pi} R_{xy}(\xi + \rho\sqrt{1+ue^{i\theta}}, \xi + \rho\sqrt{1+ue^{i\omega}})[\sqrt{1+ue^{i\theta}}, \sqrt{1+ue^{i\omega}}](1+u(\omega))\rho d\omega \\
&+ \int_0^{2\pi} R_{yx}(\xi + \rho\sqrt{1+ue^{i\theta}}, \xi + \rho\sqrt{1+ue^{i\omega}})[\sqrt{1+ue^{i\theta}}, \sqrt{1+ue^{i\omega}}](1+u(\omega))\rho d\omega \\
&+ \int_0^{2\pi} R_{yy}(\xi + \rho\sqrt{1+ue^{i\theta}}, \xi + \rho\sqrt{1+ue^{i\omega}})[\sqrt{1+ue^{i\omega}}, \sqrt{1+ue^{i\omega}}](1+u(\omega))\rho d\omega \\
&+ O(\rho^2).
\end{aligned} \tag{B.3}$$

Finally we deduce

$$\begin{aligned}
\left. \frac{\partial^4 R}{\partial \rho^4} \right|_{\rho=0} &= 12\pi R_{xx}(\xi, \xi)[\sqrt{1+ue^{i\theta}}, \sqrt{1+ue^{i\theta}}] \\
&+ 5 \int_0^{2\pi} R_{xy}(\xi, \xi)[\sqrt{1+ue^{i\theta}}, \sqrt{1+ue^{i\omega}}](1+u(\omega)) d\omega \\
&+ 3 \int_0^{2\pi} R_{yx}(\xi, \xi)[\sqrt{1+ue^{i\theta}}, \sqrt{1+ue^{i\omega}}](1+u(\omega)) d\omega \\
&+ 3 \int_0^{2\pi} R_{yy}(\xi, \xi)[\sqrt{1+ue^{i\omega}}, \sqrt{1+ue^{i\omega}}](1+u(\omega)) d\omega \\
&= 12\pi R_{xx}(\xi, \xi)[\sqrt{1+ue^{i\theta}}, \sqrt{1+ue^{i\theta}}] \\
&+ 3 \int_0^{2\pi} R_{yy}(\xi, \xi)[\sqrt{1+ue^{i\omega}}, \sqrt{1+ue^{i\omega}}](1+u(\omega)) d\omega.
\end{aligned} \tag{B.4}$$

References

- [1] F. S. Bates and G. H. Fredrickson. Block copolymers - designer soft materials. *Physics Today*, 52(2):32–38, 1999.
- [2] X. Chen and Y. Oshita. Periodicity and uniqueness of global minimizers of an energy functional containing a long-range interaction. *SIAM J. Math. Anal.*, 37(4):1299–1332, 2005.
- [3] R. Choksi and X. Ren. On the derivation of a density functional theory for microphase separation of diblock copolymers. *J. Statist. Phys.*, 113(1-2):151–176, 2003.
- [4] R. Choksi and X. Ren. Diblock copolymer - homopolymer blends: derivation of a density functional theory. *Physica D*, 203(1-2):100–119, 2005.
- [5] P. C. Fife and D. Hilhorst. The Nishiura-Ohnishi free boundary problem in the 1D case. *SIAM J. Math. Anal.*, 33(3):589–606, 2001.
- [6] A. Gierer and H. Meinhardt. A theory of biological pattern formation. *Kybernetik*, 12:30–39, 1972.
- [7] Z. Han. Asymptotic approach to singular solutions to nonlinear elliptic equations involving the critical Sobolev exponent. *Analyse Nonlinéaire*, 8(2):159–174, 1991.
- [8] T. Kolokolnikov, M. Ward, and J. Wei. Spot self-replication and dynamics for the Schnakenburg model in a two-dimensional domain. *J. Nonlinear Sci.*, to appear.
- [9] I.M. Lifshitz and V.V. Slyozov. The kinetics of precipitation from supersaturated solid solutions. *J. Phys. Chem. Solids*, 19:35–50, 1961.
- [10] B. Niethammer. Derivation of the LSW-theory for ostwald ripening by homogenization methods. *Arch. Ration. Mech. Anal.*, 147(2):119–178, 1999.
- [11] B. Niethammer and F. Otto. Ostwald ripening: the screening length revisited. *Calc. Var. and PDE*, 13(1):33–68, 2001.
- [12] Y. Nishiura and I. Ohnishi. Some mathematical aspects of the microphase separation in diblock copolymers. *Physica D*, 84(1-2):31–39, 1995.
- [13] T. Ohta and K. Kawasaki. Equilibrium morphology of block copolymer melts. *Macromolecules*, 19(10):2621–2632, 1986.
- [14] X. Ren and J. Wei. On a two-dimensional elliptic problem with large exponent in nonlinearity. *Trans. Amer. Math. Soc.*, 343(2):749–763, 1994.
- [15] X. Ren and J. Wei. Single point condensation and least-energy solutions. *Proc. Amer. Math. Soc.*, 124(1):111–120, 1996.
- [16] X. Ren and J. Wei. On the multiplicity of solutions of two nonlocal variational problems. *SIAM J. Math. Anal.*, 31(4):909–924, 2000.
- [17] X. Ren and J. Wei. Concentrically layered energy equilibria of the di-block copolymer problem. *European J. Appl. Math.*, 13(5):479–496, 2002.

- [18] X. Ren and J. Wei. On energy minimizers of the di-block copolymer problem. *Interfaces Free Bound.*, 5(2):193–238, 2003.
- [19] X. Ren and J. Wei. On the spectra of 3-D lamellar solutions of the diblock copolymer problem. *SIAM J. Math. Anal.*, 35(1):1–32, 2003.
- [20] X. Ren and J. Wei. Triblock copolymer theory: Free energy, disordered phase and weak segregation. *Physica D*, 178(1-2):103–117, 2003.
- [21] X. Ren and J. Wei. Triblock copolymer theory: Ordered ABC lamellar phase. *J. Nonlinear Sci.*, 13(2):175–208, 2003.
- [22] X. Ren and J. Wei. Stability of spot and ring solutions of the diblock copolymer equation. *J. Math. Phys.*, 45(11):4106–4133, 2004.
- [23] X. Ren and J. Wei. Wriggled lamellar solutions and their stability in the diblock copolymer problem. *SIAM J. Math. Anal.*, 37(2):455–489, 2005.
- [24] X. Ren and J. Wei. Droplet solutions in the diblock copolymer problem with skewed monomer composition. *Calc. Var. Partial Differential Equations*, 25(3):333–359, 2006.
- [25] X. Ren and J. Wei. Existence and stability of spherically layered solutions of the diblock copolymer equation. *SIAM J. Appl. Math.*, 66(3):1080–1099, 2006.
- [26] X. Ren and J. Wei. Many droplet pattern in the cylindrical phase of diblock copolymer morphology. *Rev. Math. Phys.*, 19(8):879–921, 2007.
- [27] X. Ren and J. Wei. Single droplet pattern in the cylindrical phase of diblock copolymer morphology. *J. Nonlinear Sci.*, 17(5):471–503, 2007.
- [28] X. Ren and J. Wei. Spherical solutions to a nonlocal free boundary problem from diblock copolymer morphology. *SIAM J. Math. Anal.*, 39(5):1497–1535, 2008.
- [29] O. Rey. The role of the Green’s function in a nonlinear elliptic equation involving the critical Sobolev exponent. *J. Funct. Anal.*, 89(1):1–52, 1990.
- [30] A. M. Turing. The chemical basis of morphogenesis. *Phil. Transact. Royal Soc. B*, 237(641):37–72, 1952.
- [31] C. Wagner. Theorie der Alterung von Niederschlägen durch Umlösen. *Z. Elektrochem.*, 65:581–594, 1961.